FINITE ELEMENT MODELING OF RESIDUAL STRESSES OBTAINED BY CUTTING PIECES: A REVIEW

Pavel Iurea

"Gheorghe Asachi" Technical University of Iasi, Romania, Blvd. Mangeron, No. 59A, 700050 Iasi, Romania

Corresponding author: Pavel Iurea, pavel.iurea@yahoo.com

Abstract: Knowing the size and influence of residual stresses is important both for mechanical processing and for the functioning of components and mechanical structures. The residual stresses generated in a manufacturing process are a consequence of the effects of thermo-mechanical and microstructural phenomena.
Besides experimental methods that can be used to determine residual stresses during and after the completion of a mechanical process or even after getting the final part or structure, finite element numerical method can be used before processing, so engineers have the opportunity to choose appropriate processing parameters in the production process.
This paper contains an overview of finite element analysis methods used to estimate the residual stresses in machining of steels. With specialized programs can be simulated chip removing manufacturing processes and finally can be estimated sizes and distributions of residual stresses.
During previous research using finite element analysis method, several parameters were identified as significant in the contribution of residual stress generation. Among the parameters that were proven to have the greatest influence are geometry processing tool (cutting edge radius, tool peak radius, rake angle, clearance flank wear), cutting conditions (cutting speed, feed, depth of cut) and the behavior of the workpiece (mainly its hardness)
Key words: finite element, metallic materials, parametric analysis, specific machining, residual stress.

1. INTRODUCTION

Machining is a manufacturing process used to remove the material from the workpiece (blank) in order to obtain a finite piece. Cutting processes involve a variety of physico-chemical phenomena, mechanical and structural transformations of which are mentioned: elastic-plastic deformation, thermo-mechanical effects, contact-friction conditions and mechanisms for separating chips [43, 50]. Tensions in the process of conversion are called remanent or residual stresses. Residual stresses are not irreversible. In time, or under external force (vibration, temperature, etc.) they can diminish [54]. Because the majority machining phenomena occur at low depth compared to the workpiece surface, residual stresses are located mainly in the surface layer, and in layers close [20].
Usually, the absolute value of the residual stress near the surface of the workpiece is large and decreases with increasing depth (Figure 1).
The residual stresses in the surface layer are an important factor in determining the performance and fatigue life of components. Reducing residual stresses determines mainly dimensional changes in the shape and mutual position of surfaces, that can change the functional conditions of the assembly to which the piece belongs.
Studies on residual stresses have provided important information on these events and the distribution of residual stress [20]. These studies have analyzed the influence of workpiece material, the working parameters, cutting tool and cutting conditions [20].
In the scientific literature the residual stresses and their effects were studied by experimental and analytical methods.

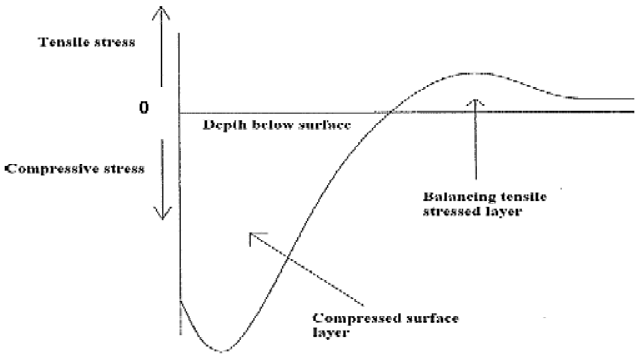

Fig .1 Distribution of residual stresses depending on the depth of processed surface [20]

Analytical research methods are exact and numerical methods. Accurate methods are difficult if not impossible to apply therefore have been developed a series of numerical methods such as finite element method (FEM).
The finite element method is a very convenient way to obtain approximate solutions for almost any engineering problemthus becoming a convenient and necessary tool in the design and research calculations [53]. Merwin

and Johnson [23] proposed a method for modeling which was used to estimate the residual stress produced in the processing. The first FEM analysis to estimate the residual stress that may occur in the processing was performed by Okushima and Kakino [32].
The application of FEM modeling of residual stress use specific computer applications (developed on the issue) or general applications (commercial) of finite element made by large IT companies: Ansys, Abaqus, Deform, AdvantEdge, Nastran, Cosmos, Algor etc.

2. THE CAUSES OF THE GENERATION OF RESIDUAL STRESSES IN MACHINING

Arboform The main causes of the generation of residual stresses are plastic deformation, thermal requests and phase transformation of the material machined surface.
It is commonly recognized that tensile residual stresses occur after heating the machined surface during cutting operation [25]. The high value of the temperature of a thin layer near the surface heat affected part, cause thermal expansion and plastic flow.
During the successive cooling, thermal shrinkage of this layer is higher than the rest of the part, and this phenomenon is considered to be the origin of the tensile residual stress generated in the process [25]. Most research has shown that in the absence of the thermal solicitations, mechanical load exerted on the workpiece leads to the appearance of compressive residual stress.
In some studies [8], several parameters were identified as significant for the residual stress generation. Among the parameters that have proved to have a great influence are the geometry of the processing tool (radius of the cutting edge, radius at the top of the tool, rake angle, machining tool wear - especially clearance of the face), cutting conditions (cutting speed, feed, depth of cut), tool/splinter and interface tool/machined material contact conditions, properties of the workpiece and machining tool material.
In the case of turning of the steel roughing are induced compressive residual stresses at the surface and inside the workpiece, thereby increasing the resistance to fatigue [3], which is particularly useful for parts with rotational motion under external loads, such as bearings. High temperatures and rapid cooling in the area of chip removal can produce phase transformations in the superficial layer, generating a thin layer of tempered martensite known as white layer [12]. As a consequence of this transformation, in this layer, another layer may be formed, called black layer of lower hardness, and which is subjected to residual stresses. According to the reference [45], one of the main factors of generating of these layersis cutting tool wear, which is a critical factor in increasing the temperature in the area of chip removal.
Processing conditions (working parameters) also produce residual stresses in the workpiece and are an important factor to be considered especially when there are repeated requests, existing many studies in this field [8,9,44,52]. Depending on the values of residual stresses existing in the material, the duration of life of a bearing can be increased to more than 30% [59].
Hard turning operations [2], two major factors influence the resulted residual stress. First, the cutting force produces local plastic deformation which tends to induce compressive residual stresses. Secondly, the high temperatures resulted from plastic deformation and friction at the tool-piece can cause tensile residual stresses and phase transformations that generate white layer, as mentioned above. Tensile residual stresses and white layer are detrimental to the life of the machined parts, because it favors the formation of cracks and their propagation thus resulting in breakage of parts.

3. THEORIES ON THE MODELING OF RESIDUAL STRESSES

Most studies have provided results regarding the influence of the mechanical and thermal loads on the size, type and residual stress distribution. In these studies, the most used methods were based on finite element analysis [21, 22]. For residual stress analysis in orthogonal cutting of AISI 1045 and AISI 316L steel, Outeiro et. al. [34, 56], Nasr et al. [29] and Salio et al. [55], were used the finite element method. The results obtained were compared with the experimental results of M'Saoubi et al. [57]. After thease were analyzed the effect of sequential cuts and the influence of the cutting tool [33, 46].
In some papers [25] it is shown that in the absence of thermal effects, a substantial level of tensile residual stresses can be obtained only by purely mechanical effects. The result leads to reconsideration of residual stresses modeling methods through the possibility of systematic analysis in which to study the influence of each parameter separately. This is possible through finite element analysis, after successive examining of each parameter, to estimate its effects.
In the research belonging to Wiesner [51] finite element method was used to determine residual stress in orthogonal machining of AISI 304 steel, with the objective of determining the interaction between thermal loads and cutting forces. The model results showed that the thermal and mechanical regime of the orthogonal cutting process causes tensile residual stresses. The model was validated by X-ray diffraction measurements of the processed sample. Small shear angles and functional angles of the cutting tool proved to be the factors that have

increased the tensile residual stress.

Methods of modeling residual stresses

Some papers have approached through the finite element the following models: linear and nonlinear elastic model, elasto-plastic model, visco-plastic model, thermal phenomena, etc. At the simulation of metalworking, the formulations of finite elements models [41] are based on implicit or explicit schemes. The implicit scheme requires a convergence of integration at each time step, that provides better accuracy, but due to restrictive contact conditions, appear a higher level of complexity at discontinuous chip formation. The explicit scheme solve the system of equations using the informations from the previous stages. This scheme was used in metal processing involving large and complexes non-linearities of frictional conditions on contact. The main methods used in finite element analysis of metal cutting, are Lagrange and Eulerian. Based on the mains advantages of the first two methods researchers have developed new methods: the Lagrangian-Eulerian arbitrary formulation and the Lagrange updated formulation.

Lagrange method

Lagrange method assumes that the finite element eye is attached to the workpiece material and follows its deformation, stress calculation being done gradually and deformations incrementation and the updating of the nodal coordinates are made after each incremented stage. Lagrange method is widely used because of its ability to form chips and determine the splinters geometry depending on the chip removal parameters of the plastic deformation and material properties. The disadvantage of this method is the severe plastic deformation which occurs in the material due to element deformation, requiring a new discretization (less dense) of the elements. Also it must be defined a separating criterion for the chip, the parameters estimation of this criterion being a difficult task, due to lack of data. Lagrange method deficiencies can be eliminated by using an updated Lagrange method that allows automated rediscretization technique.

Eulerian method

In Eularian method the possibility of element deformation throughout the process is eliminated by the finite element eye fixed in space and by the material flow through the front of the element. Are required fewer elements analysis due to processed material condition equilibrium, leading to a reduced computation time. In case of Eulerian models for defining rupture chip, do not need a separation criterion of this. The drawback of Eulerian method is the need for prior knowledge of chip-tool contact length and contact conditions; the chips geometry. This disadvantage can be overcomed, using an iterative procedure to adjust the chip-tool contact length and the geometry of the cutting.

Arbitration ALE method (Lagrange-Eulerian)

This arbitrary method Lagrange and Eulerian (ALE) was proposed after the combination of the best features of classical methods. These new approach methods are applied sequentially. For displacements, severe deformation of the element was eliminated due to the finite element eye that follows the flow of material, problem solved with Lagrange, while for speeds, the problem is solved with Eulerian, discretized element eye being repositioned. The combined formulation is used in the analysis to avoid severe distortion of the element, which is a typical Lagrange problem, as well as to remove the rediscretizations frequency, in which case the Eulerian approach is used around the chip removal tool tip where the process takes place. An explanation demonstrative of the methods Eulerian, Lagrange and ALE (Lagrange-Eulerian) is shown in Figure 4 and Figure 5 presents a comparison between a discretization produced by Lagrange method (left) and a discretization produced by ALE method (the right) [14].

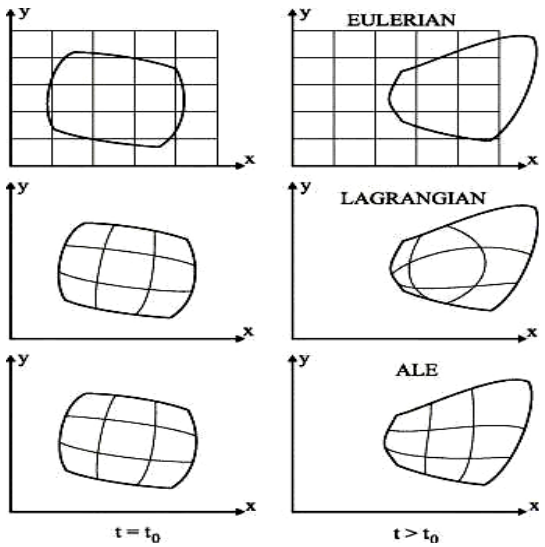

Fig. 2 A demonstrative explanation of Eulerian, Lagrange and ALE methods [41]

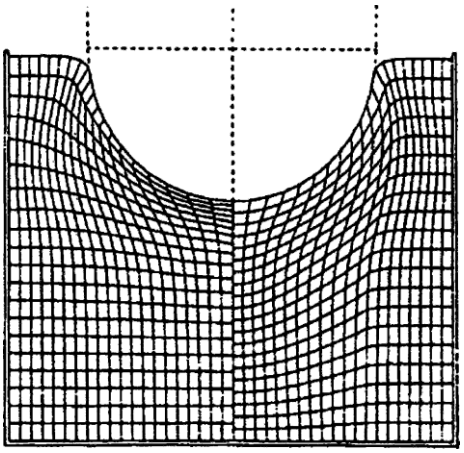

Fig. 3 Comparison of a discretization produced by Lagrange method (left) and a discretization produced by ALE method (right) [14]

Updated Lagrange method

In an attempt to overcome the disadvantages of traditional methods was developed the updated Lagrange method, recommended in case of large deformations. In this approach, the element deformation problem is solved by automated rediscretization technique and discretization eyes adaptivity. The finite element eye, the local reference frame and the local coordinates of the element are continually updated. The high time calculation represents the main disadvantage of the proposed method.

4. FINITE ELEMENT MODELING OF RESIDUAL STRESSES

The numerical modeling method FEM can accurately estimate the residual stresses induced in machined surfaces. For best estimates and reliable results of residual stress distribution in a machined surface, the main aspects that can be considered for the FEM simulation models are: workpiece model, friction model and chip separation criteria (breaking criterion).

The workpiece model should represent satisfactorily the elastic-plastic and thermomechanical behavior of the workpiece deformations observed during machining process. The accurate and reliable models of the continuous stress flow are considered extremely necessary to represent the constitutive behavior of the workpiece in high speed cutting conditions. The modeling stress flow of the workpiece material is one of the most important aspects in considering the simulation of metal cutting process. The stress flow is the instantaneous value of flow and is represented mathematically by the constitutive equations, depending on the deformation, the deformation and temperature size. Among the constitutive material models are widely used Oxley, Johnson - Cook and Zerilli - Armstrong. In specialized literature, studies have favored the use of Johnson - Cook constitutive material model and among them are Umbrello et al., Özel and Zeren [39], Outeiro et al. [37] Liang Su [15]. The model material Johnson - Cook is one constituent that at large deformations contains high values of demands and high temperatures. The developed model is well suited for the calculation of processing through the use of variables that are available in most of the computer codes applicable to FEM. Torsion tests on a wide range of types of requests on tensile, tensile static tests, tensile dynamic tests of the Hopkinson bars and Hopkinson bar tests at elevated temperatures are used to obtain the necessary data for the material constants.

The constituent material model Johnson - Cook is expressed as,

$$\bar{\sigma} = (A + B\bar{\varepsilon}^{n})\left(1 + C\ln\left(\frac{\dot{\bar{\varepsilon}}}{\dot{\bar{\varepsilon}}_0}\right)\right)\left(\frac{\dot{\bar{\varepsilon}}}{\dot{\bar{\varepsilon}}_0}\right)^{\infty}(1 - T^{*m}) \quad (1)$$

$$T^{*} = \frac{(T - T_{room})}{(T_{melt} - T_{room})} \quad (2)$$

where:

ε is the equivalent plastic deformation, $\left(\frac{\dot{\bar{\varepsilon}}}{\dot{\bar{\varepsilon}}_0}\right)$ is the dimensionless rate of plastic deformation, T* is the homologous temperature. The five material constants are A, B, n, C and m. The expression in the first set of brackets represents stress depending on the deformation. The expressions in the second and third set of brackets represent the effects of deformation rate and temperature, respectively. A is flow limit and B and n are the deformation effects. C is a constant deformation rate. T is the instantaneous temperature, Troom is the room temperature, and Tmelt is melting temperature of a given material. The simulation of physical processes around the cutting edge radius of the tool should not be distorted by the criterion of separation chip in the FEM model especially when the tool edge geometry is presented as a round edge or beveled edge. From the point of view of the process, breaking criterion allows the prediction of the geometry of the tool, however, the prediction criteria influencing forces and other parameters. In processing, large deformations occur, prediction and control of material breakage is a critical issue. In order to investigate the finished surface and the integrity of the manufactured piece , damage and breakage of the material must be considered. In the numerical model, the rupture was simulated by either removing the discretization elements that have been subjected to high deformation and stress or by separation element nodes (Figure 4).

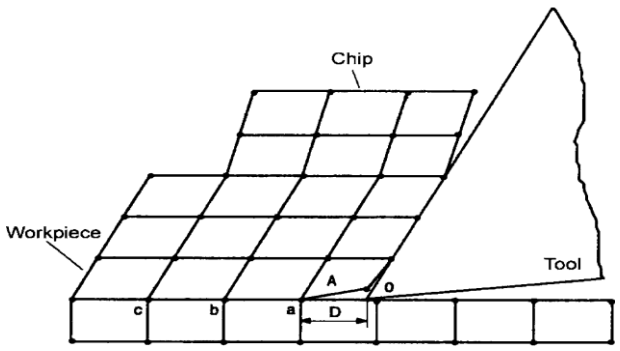

Fig. 4. The separation nodes at the distance D between the tool cutting edge (point O) and the next node (node A) [3]

A critical value of damage is defined for a given breaking criterion and when this value is reached, fracture occurs. Breaking criterion is applicable to a wide range of load conditions and processes of machining, due to the ease in calculation of the numerical.

Failure criterion is expressed by the following statement:

$$\int^{\bar{\varepsilon}_l} \frac{\sigma^*}{\bar{\sigma}} d\bar{\varepsilon} \qquad (3)$$

Where:

σ* is the main tensile maximum stress, and $\bar{\varepsilon}_l$ deformation at break. Effective stress and deformation are represented by $\bar{\sigma}$ and respectively $\bar{\varepsilon}$.

In addition, it should be noted that friction is one of the most important phenomena in the simulation machining. Özel and Zeren [39] stated that cutting metal friction plays an important role in thermo-mechanical flow of chips and the integrity of the machined surface. In the first analysis of metal processing, the Coulomb simple model friction was considered throughout the contact area at the interface tool-chip. Friction stresses are assumed proportional to the normal stress using a constant friction coefficient μ.

The model is defined as,

$$\tau = \mu\sigma_n \qquad (4)$$

where:

τ is tensile stress and σ_n is the normal stress.

The constant shear model is another friction model. The model assumes that when a constant friction stress is assumed on the rake face, low-voltage variations τ with σ_n are neglected.

Friction stress is equal to a fixed percentage of the flow shear stress of the workpiece. The model is expressed by the following relationship:

$$\tau = mk \qquad (5)$$

where m is the friction factor.

In the works of Filice et. al. [11] and Özel [38], was proposed a more realistic model proposed by Zorev, which considered the tool rake face as being divided into two areas of friction. In the first area (Figure 5), assumed to be constant and equal to the shear stress known as the bonding zone, the friction stress is

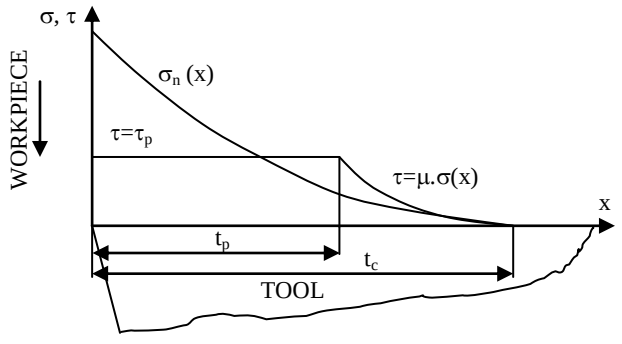

Fig.5 The distribution of stress voltage on the rake face [41]

of the flowing material (the normal stress is very high). In the second region, named the sliding zone, the normal stress is low. The model suggests that the normal stress decreases from the cutting edge of the tool to the point where the chip is separated from the tool.

The bonding zone is modeled through the constant shearing friction model and the sliding zone is modeled by Coulomb friction model. The model can be expressed by the following formulations:

$$\begin{aligned} &\tau(x) = \mu\sigma_n(x) \quad when \tau < k, \\ &\tau(x) = k \quad when \tau \geq k. \end{aligned} \qquad (6)$$

In their study on the analysis of friction modeling in orthogonal machining, Filice et al. [11] concluded that the main mechanical results such as contact length, forces, etc., are not sensitive to the friction model. The friction model is more relevant to thermal analysis. Özel [38], using finite element simulation of machining, studied the influence of friction models measured on normal and friction stress on the tool rake face are more accurate. He noted that friction models have a significant influence on the prediction of cutting geometry, forces and tensions from the cutting tool.

Estimates exact simulation of stress and temperature distributions can be obtained when in the case of a processed material are essential for tool-splinter interface, stress flow model, a suitable criterion for breaking and suitable friction model. Further studies of simulation can be also performed to identify the optimal geometry of the cutting tool edge and the process conditions to obtain the best surface integrity, longest lifetime of the obtained component and the tool with the highest productivity.

The success and reliability of numerical simulations are largely dependent on correct selection of mechanical and thermo-physical properties of the workpiece and also of the tool- splinter contact conditions and tool-workpiece interface. This is considered a critical step for acceptable accuracy to be estimated residual stresses.

In [25] Miguel and others have developed an A.L.E. model of flat deformation to orthogonal cutting using ABAQUS/Explicit commercial code with finite element. The main objective is to understand and quantify how much residual stresses are influenced by mechanical parameters. It was taken into consideration the influence of thermo-mechanical coupling parameters, such as thermal expansion, thermal soaking, Taylor-Quinney coefficient (proportionally characterized by plastic deformation converted into heat) and coefficient of friction (friction heating control). The effects of the geometry of the tool, such as the tool rake angle and the radius of the tip of the tool are also analyzed. There are

taken into consideration also the dry cutting conditions and the Coulomb friction coefficient. The friction coefficient has a complex effect by controlling heat generation along the clearance faces and settlement of cutting tool and the tendency to remain attached to the tool.

It was analyzed how residual stresses are affected by the interaction of these phenomena. Basic model geometry (rake angle of zero, cutting edge radius 0.02 mm) was modified to analyze different undercuts of the tool (zero, positive and negative) and various top radii of the cutting edge (from 0.02 to 0.15 mm). One of the requirements of the model is to avoid distortion of the network's elements at high friction conditions. A specific network is defined for a given tool geometry and is used to perform all calculations related to the geometry. This requirement is useful to avoid the influence of other factors related to numerical modeling, such as the size of the network elements. A coupled thermomechanical analysis was developed, with the type of element CPE4RT (see ABAQUS/ Explicit manual). These are the plan of deformation, quadrilateral, linearly interpolated and thermally coupled elements with reduced integration and automatic control, for the A.L.E. formulation. The analysis was performed in two steps. In the first step, the cut has been shaped at constant cutting speed and steady state conditions were reached. In the second step, the workpiece has been discharged and cooled. Residual stress distribution was obtained in a section of the piece corresponding to stationary conditions during cutting. The characteristics of the numerical model are shown in Figure 6. The tool is fixed and the cutting speed is applied to the workpiece. Cutting takes place in the plane 1-2, under plane stress conditions. The splinters formation supposedly continues. Many A.L.E. models developed in the specialized literature which requires the Eulerian contours, allowing the material to flow in a similar manner as the fluid [24, 40].

The objective of the simulation being to obtain the residual stress distribution, the model should include the unloading and cooling stages. In this case, the A.L.E. model should use Lagrange slipping and contours, making possible the flow of material over an Eulerian internal area surrounding the tool tip. This approach avoids the extreme distortion of network elements, allowing the simulation of processes involving different friction coefficients with the same initial network.

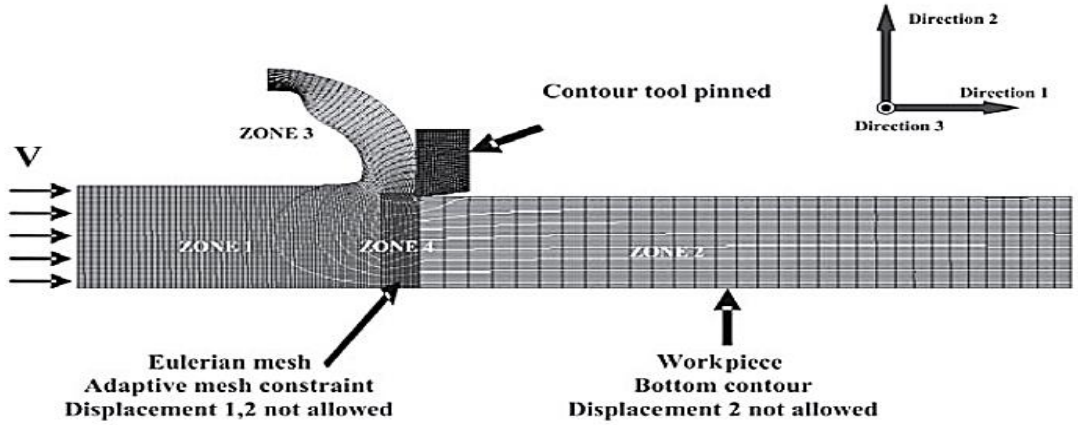

Fig. 6 The geometry model and the contour conditions **[**25**]**

The A.L.E. model was divided into several areas that allow network elements movement or material flow over the fixed network, depending on the area that is considered in the model. Areas 1, 2 and 3 combine the Lagrange limits with sliding limits (if the material flow can be tangent to the contour, but it can not go beyond this limit). Area 4 is an Eulerian region with fixed network elements, allowing the material flow over the region. The main advantage of this technique is that the distortion is avoided in the region around the tool tip with no separation criterion, which is always an artificial parameter in the Lagrange model. Another advantage is that it is not necessary to establish the line of separation, allowing for example the simulation of tools with negative rake angles. However segmentation splinters can not be shaped with this technique. Therefore, this model could become unrealistic when high speed segmentation splinters processing is simulated or heat-resistant alloys are studied. Another disadvantage is the initial definition of the splinters. Although the uncut splinters form is previously analysis defined, splinter formation during cutting and the distorting element level depend strongly on simulation parameters (for example, of friction coefficient). The main problem is to determine the tool geometry given (after some simulations) by initial network, which will be later used for different values of material parameters. These geometries were defined according to the characteristics of the instruments considered in the numerical simulations. The physical properties of the tool material and the workpiece material were found

in the recent work [31] and are summarized in Table 1 and Table 2. The material of the blank is a tube of AISI 316L with a wall thickness of 2 mm. The support tool (Figure 7a) was instrumented with strain gauges to measure cutting forces during orthogonal cutting of the tube. Several simulations were performed with the proposed constitutive equations in Table 1, and results of cutting force are shown in Figure 7b, which shows the the good estimation of the cutting force with selected constituent equation.

Table 1. Three sets of constants Johnson - Cook of material for AISI 316L steel [5]:

Reference	A (MPa)	B (MPa)	n	C	m	$\dot{\varepsilon}_0\left(s^{-1}\right)$
Chandrasekaran et al. 1	305	1161	0.610	0.010	0.517	1
Chandrasekaran et al. 2	305	441	0.100	0.057	1.041	1
Tounsi et al.	514	514	0.508	0.042	0.533	10^{-3}
Present work	400	750	0.500	0.040	0.500	1

Table 2. Reference properties for K313 (tool manufacturing) and AISI 316L (workpiece material) [31]

Property	K313	AISI 316L
Moduls of elasticity (GPa)	615	193
Poisson's ratio	0.22	0.3
Density (kg/m^3)	14900	8000
Specific heat capacity (J/kgK)	138	500
Thermal conductivity (W/mK)	79	20
Linear coefficient of thermal expansion (mm/mmK)	-	19.9E-6

The model was validated by comparing the residual stress field obtained numerically with the experimental data reported in the literature. Model conditions for validation were: departure angle is zero, the cutting edge radius R = 0.02mm, cutting speed v = 100 m / min, the friction coefficient μ = 0.2, feed rate = 0.1 mm / rev. The experimental results have been obtained by M'Saoubi et al. [57]. The authors replicated orthogonal cutting conditions obtained at turning tests. Figure 7 shows the correlation between numerical and experimental results.

After measuring cutting forces and residual stresses from the literature, it was concluded that the values of material parameters given in Table 1 are representative for the thermomechanical properties of AISI 316L steel. This set of parameters can characterize reference material in parametric analyzes performed in various works.

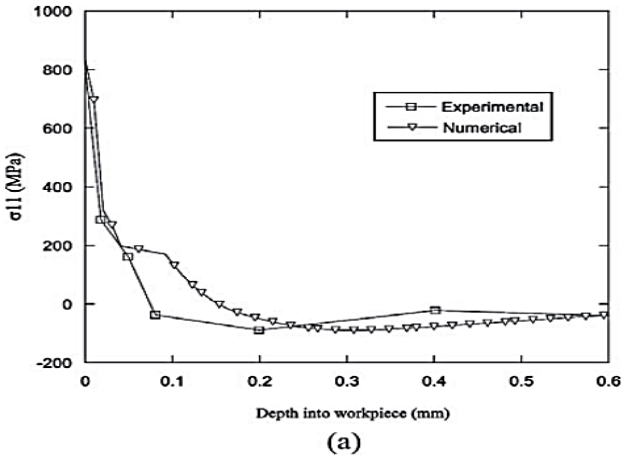

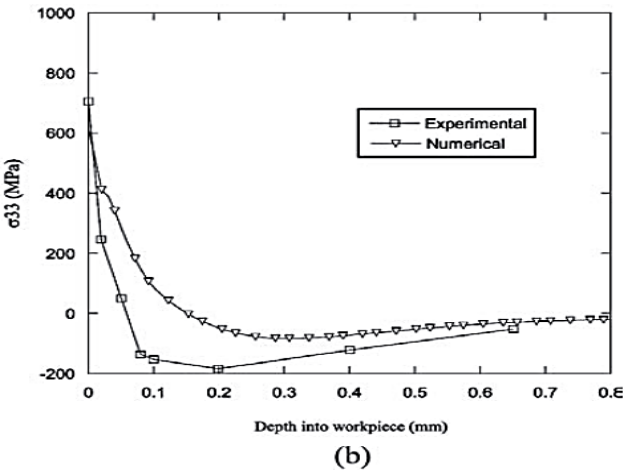

Fig. 7. Experimental validation of the model. Residual stress distribution after testing AISI 316L steel at cutting speed of 100 m/ min. σ 11 is the radial tension (a), σ 33 is the axial tension (b) [25, 36, 57]

Abboud et al. [1] have developed a finite element model coupled thermo-mechanical of the orthogonal cutting process using Deform-2D program to estimate the residual stresses and machining forces and temperatures for Ti-6Al-4 titanium alloy, processed with sharp tools from uncovered carbide. It was investigated the residual stress behavior generated in the processing of titanium alloy depending on the deformations, the advance and temperature. The workpiece was defined as an elastomeric plastic body being discretized into 2500 linear quadrilateral elements with 4 nodes of integration. The data generated were used to model the behavior of the stress generated in the workpiece in accordance with the combined effect of deformation, deformations size and temperature. The cutting tool was defined as

a rigid body discretized into 2500 linear quadrilateral elements with 4 nodes. It were used a heat transfer coefficient of 105 kW / m 2 ° C [42] and a friction coefficient m = 0.9. The shape of the chips was modeled continuously to study turning finishing regime. The established model and contour conditions are described in Figure 8.

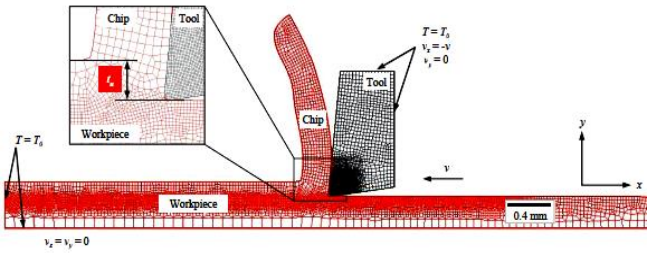

Fig. 8. Configuring the 2D finite element model and contour conditions [1]

The workpiece and tool edges that are far from the cutting area were stored at ambient temperature T_0 = 20 °C. To experimentally validate the FEM model were made orthogonal cutting tests using a Boehringer NG 200 turning center equipped with a Kistler 912 dynamometer. The cutting was performed with cutting tools with uncoated carbide of Kennametal K68 quality. Processed samples consisted in bars of 50 mm diameter Ti - 6Al - 4V steel, processed at one end. The surface residual stresses in direction of the cut (x) have been measured using the technique of X-ray diffraction. Surface residual stress, the range of parameters investigated was compression. A comparison between FEM predictions and experimental (EXP), measurements of cutting force (Fx), feed force (Fy) and residual surface tension (σ_x), is shown in Figure 9 for different test conditions.

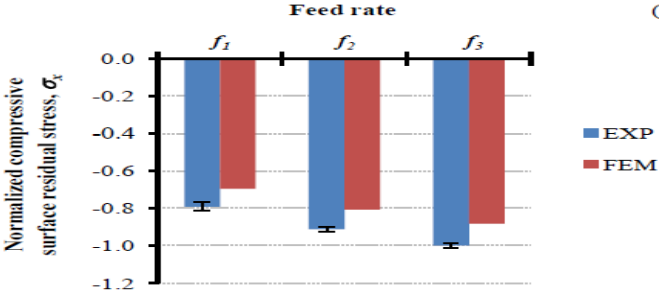

Fig. 9. Surface residual stresses in the direction of the cutting. Comparison between expected and experimental results at cutting speed v1, so that (v1 <v2 <v3) and (f1 <f2 <F3) [1]

Feed rate had a significant effect on the size and nature of the surface residual stress. By increasing the feed rate, compressive residual stress values increased. Chen et al. [7] showed that at high cutting speed conditions, the incorporation of a breaking criterion for segmented splinter in the FEM model can lead to a decrease in the processed surface temperature, coupled with an increase in compressive residual stresses estimated by FEM simulations.

A hybrid finite element model was developed by Anurag et al. [2] with the concept of cutting depth to predict residual stress profiles in hard turning. Using thermo-mechanical properties of the the workpiece, the residual stress was estimated by simulating the dynamic turning process, followed by a quasi-static process of relaxation of tension. The profiles of residual stress were estimated for a range of cutting depth encountered in processing. Residual stress profiles were estimated in agreement with the experimental ones. The effects of cutting speed, the coefficient of friction and inelastic thermal coefficient on the residual stresses were also studied and explained. In processing, when the tool advances into the workpiece in cutting direction to form a splinter, it exerts tremendous pressure on the workpiece in the cutting directionas well as a significant amount of traction in the downward direction. The cutting force partially deforms the workpiece to separate itself as a chip on the tool rake face. Pushing force causes the material to flow under the cutting edge of the tool. The point where the flow of material separates to form the splinter and the machined surface is known as stagnation point [2].

The chipped material, under the action of tool and high temperatures, suffers a severe plastic deformation, and forms the superficial layer of the processed surface. The integrity of the machined surface of the piece is determined by the state of deformation of the splinters thin layer. The amount of chipped material under the cutting edge is highly dependent on the geometry of the cutting edge of the cutting tool. The state of tension, temperatures during cutting and residual stresses after cutting is significantly determined by the amount of chipped material. Therefore, the cutting depth is believed to be the most important factor for the formation of the residual stress profile, while the splinters formation region may contribute less (about 10-20%).

In Figure 10 is presented a schematic relationship between stagnation point and the radius of the tool cutting edge. Point O is the center of the cutting edge radius, point A is the position in which the splinter comes out from the tool rake surface and point B is where the machined surface is separated from the surface of the tool sitting area. BD is ideal separation line. Actual thickness of the uncut chip and the ideal thickness of the uncut chip are t_1 and t_2 respectively. The tool edge radius is r and the chamfer angle is θ. The pitch angle is α. VB is the wear flank of the tool face sitting. The plowed depth can be expressed:

$$\delta = t_2 - t_2 = r(1-\cos\alpha) \qquad (7)$$

The value of δ represents the thickness of the amount of material that cuts through under the cutting edge of the tool to form the machined surface. According to relation (7), if the stting angle α is known, the value of δ material can be determined knowing the tool cutting edge radius r.

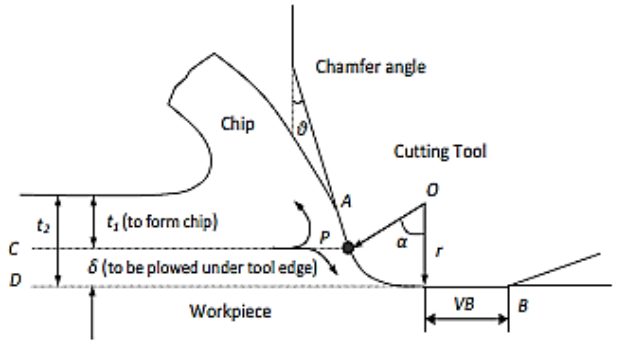

Fig . 10 The plowed depth when cutting [2]

For most materials and cutting conditions, sitting angle α varies within a certain range [2]. According to the hypothesis, the formation area of the chips (above the line PC) should contribute less to the generation of residual stresses and, therefore, it was not been shaped. Only the cutting depth (below the PC) has been shaped and simulated. Therefore workpiece discretization is designed for the plowed depth of the cutting where δ is defined by the stagnation angle α. To achieve continuous plowing on the length of the workpiece and eliminate possible severe deformations of the elements in the depth of cut, the adaptive discretization model was used to facilitate nodes and elements to adapt to deformation without affecting the accuracy of numerical simulations.

The developed temperatures that occur during processing operations are mainly related to the contact between the tool and chip, the cutting forces level and friction between the tool and chip. Part of the heat which occurs is transferred to the workpiece and cutting tool while most of it is dissipated through the splinter. Shear zone is determined mainly by the heat, therefore, the length of contact between the splinter and the tool influences the cutting forces, cutting conditions of the tool, performance and tool life.

Liu and Guo [17] used the commercial FEM code, Abaqus / Explicit, to investigate the effect of sequential cuts and tool - splinter friction on the residual stresses in a machined layer of AISI 304 stainless steel. The damage of the layer from the first splinting was found as a change in the residual stress distribution caused by the second splinting. In addition, residual voltage is sensitive to interface friction conditions splinter tool.

Umbrello et al. [49] presented a new numerical and experimental approach to estimate the residual stresses by incorporating microstructural phase transformations induced during machining AISI 52100 steel. Roughing processing AISI 52100 bearing steel is a typical case in which microstructural phenomena associated with the formation of black and white layers influences the distribution of residual stresses. Nasr et al. [30] describe a time-efficient approach to finite element (FEM) to estimate the residual stresses induced in processing using commercial software ABAQUS.

This approach reduces the computation time to estimate the residual stress of the order of days to a few minutes, which is a significant contribution in the field of metal processing and applications of finite element analysis. This approach reduces the computation time to estimate the residual stress of the order of days to a few minutes, which is a significant contribution in the field of metal processing and applications of finite element analysis. Four different processed materials were used to validate the current work by comparing the expected residual stress profiles with experimental profiles, which were obtained in similar conditions by splintering.

Mishra [58] developed a numerical model based on FEM to determine the residual stresses due to a moving heat source. The model predicted residual stresses of thermal and mechanical origin in rectification process. The author examined the effects of mechanical cutting force size, the heat input and the feed speed of the workpiece on the residual stress.

In tests conducted by Capello [4], the influence of feed rate and the edge radius at the top of the cutting tool was reported to have an impact on surface residual stresses. In general, advance growth generates significantly higher compressive stress. Gunnberg et al. [13] concluded that higher splintering speeds lead to increased tensile residual stress on the surface and the higher cutting speeds have higher values the generated heat does not penetrate deeper into the workpiece.

Gunnberg et al. [13] concluded that at advance growth and negative rake angles is generated higher compressive stress. However, feed and cutting tool edge radius has the greatest effect on the surface residual stress distribution and values. Advance growth generates significantly higher compressive stress [4]. Capello [4] concluded that a material with higher mechanical properties will present higher residual stress (more traction). The author has verified once again that the influence of process parameters on residual stress is as follows: feed rate, cutting tool edge radius and, to a lesser degree departure angle. Splinting depth, on the contrary, does not seem to influence the residual stresses. Also, cutting speed and primary angle plays a minor role. Therefore, we can say that the key parameters that control residual stresses at the mechanical processing are feed rate and cutting tool tip edge radius. Several researchers have shown that these

results are consistent to three steels investigated, suggesting that the generation of residual stress is influenced by process parameters in a common way. [4] In dry machining of stainless steel (AISI 316) was used a cement coating carbide cutting tool. Umbrello et al. [48] was used the constitutive equation (J-C), in modeling with finite element of orthogonal cutting of AISI 316L steel and predicted the cutting forces, cutting morphology, temperature distributions and residual stresses, using the effects of five different sets of Johnson-Cook material constants. According to the presented studies, residual stresses are very sensitive to J-C material constants.

Experimental and analytical results concerning the precision of turning for AISI D2 steel, was compared with the modeling simulations with finite element by Davim et al. [19]. The differences between the experimental results (analytical calculations) and numerical simulations suggest that the finite element method has reasonable accurate estimates. Outeiro et al. [35] showed that the residual stress is one of the most relevant parameters used for evaluation of machined surfaces in case of the processing of critical structural components with high demands for reliability. The high level of tensile residual stress (sometimes reaching over 1000 MPa), is generated in the machined surface by the higher cutting forces produced with high temperatures localized around cutting edge. During machining AISI 316L steel, residual stresses generated are usually machined surface traction and high compressive layer below the surface [34]. Residual stresses generated during the processing of nickel based alloys such as Inconel 718, are even more critical. This material is mainly used in the aerospace industry to produce engine components due to its ability to withstand to high loads under aggressive environments (high temperatures, corrosion, etc.). Tensile residual stresses induced by processing of such alloys are of the same order of magnitude as, or sometimes even higher than those of residual stress induced by machining steel AISI 316L. In Table 3 are presented the geometry of coated and uncoated cement carbide tools and cutting parameters for the analysis of residual stresses induced by dry turning of AISI 316L steel and Inconel 718 alloy.

The influence of process parameters reduction on the processing performance and surface integrity generated during dry turning of AISI 316L austenitic stainless steel with coated and uncoated carbide and Inconel 718 steel was studied by Outeiro and colab. [35]. To simulate the cutting process for AISI 316L steel and Inconel 718 alloy, was used a commercial FEA software Deform - 3DTM version 6.1 and a default Lagrange code. For dry turning operation was developed a finite element model, composed of the workpiece and tool, that is presented in Figure 11.

Table 3. Tool geometry and cutting parameters (C - covered, U-uncovered) [35]

	T_1(C, U)	T_2(U)
Tool cutting edge radius, r_n (µm)	25	44
Tool nose radius, r_ε (mm)	0.8	0.8
Normal rake angle, y_n (°)	-6	-4.29
Normal flank angle, α_n (°)	6	4.29
Inclination angle cutting edge, λ_s (°)	-6	-14
Tool cutting edge angle, k_r (°)	95	72
Tool minor cutting edge angle, k'_r (°)	5	72
Cutting speed, v_c (m/min)	55; 70	125
Feed, f (mm/rev)	0.15; 0.2	0.05
Depth og cut, a_p (mm)	0.5	2.5

For the begining the tool was modeled as rigid and the workpiece was discretized by 180 000 quadrilateral isoparametrics elements. It was performed the analysis of a plan of coupled thermo-mechanical deformation. From Deform database were used the data for to model the behavior of thermo-elastic-viscoplastic Inconel 718 alloy.

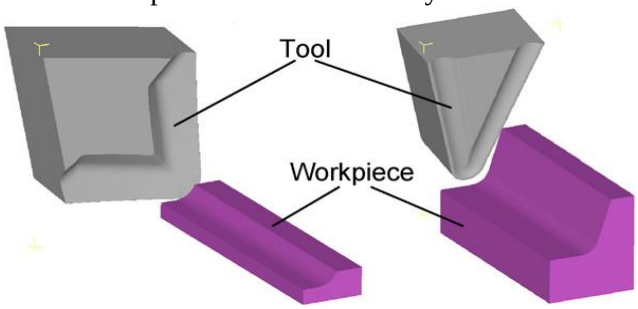

Fig. 11 FEM analysis of of cutting tool geometry turning to the operation (tool geometry on the left - T1, geometry tool on the right- T2 [35]

The elastic behavior of AISI 316L steel, was modeled using data presented in Outeiro studies [33].The thermo-viscoelastic behavior of AISI 316L steel, was shaped using Johnson-Cook constitutive equation (for material constants) [37]. From Deform database was used the physical properties of Inconel 718 and AISI 316L steels and thermal conductivity of the cutting tool pils.

5. INFLUENCE OF OPERATING PARAMETERS ON THE DISTRIBUTION AND SIZE OF RESIDUAL STRESSES

The influence of processing parameters on the surface integrity and especially on the residual stresses generated during processing was mentioned using the numerical methods, in several works from the specialized literature. A powerful tool to analyze the effect of different factors involved in the generation of residual stresses is FEM. For investigation of the effect of cutting speed on the residual stress induced under the surface area after orthogonal cutting, Mohammadpour et al. was used [27] a finite element analysis using a nonlinear finite element model called

Superform. Finally, FEM modeling results were compared with experimental measurements found in the literature regarding the orthogonal cutting of AISI 1045 steel, concluding that these data are in good agreement. The residual stress distribution (Figure 12) over cutting process of AISI 316 stainless steel, was simulated FEM analysis. The feed rate had three different values, 0.05, 0.1 and 0.2 mm/rev, cutting spead being 100 m/ min and cutting depth of 1 mm. For this study was used AdvantedgeTM program. At AISI 316 blank processing, were used tools from materials coated and uncoated with cemented carbide. The maximum tensile residual stress has similar values for all feed rate values (ranging from 250 to 300 MPa). the same can be said for the compressive residual stresses differ for these three values of feed rate, -100 MPa for a feed rate of 0.05mm / rev, -150 MPa for a feed rate of 0.1 mm / rev and -200 MPa for a feed rate of 0.2 mm / rev.

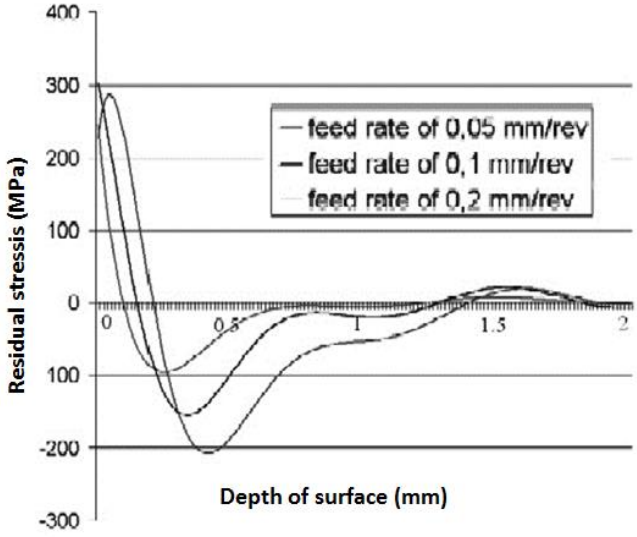

Fig . 12 The distribution of the residual stress on the surface depth for AISI 316 steel, depending on the speed of advance [19,20]

These values were at a depth of 0.26 mm, 0.35 mm and 0.42 mm respectively. For tensile residual stresses from the surface layer, depth of surface increase with feed rate being approximately 0.1mm for a feed rate of 0.05 mm / rev, about 0.17 mm for a feed rate of 0.1 mm / rev and 0.2mm for a feed rate of 0.2mm / rev [19]. The analyze of different values effect of cutting speed on the residual stress, cutting forces and temperatures with a constant feed rate and a sharp cutting edge of the tool, was realized using FEM method by Abboud et al. [1]. While cutting speed range At experimental investigation, cutting spead was between (20-90) m / min, and for numerical investigation values in the range of (100-274) m / min. Figure 13 show The effect of cutting speed on the surface residual stresses and on the cutting force (Fx) in the direction (x).

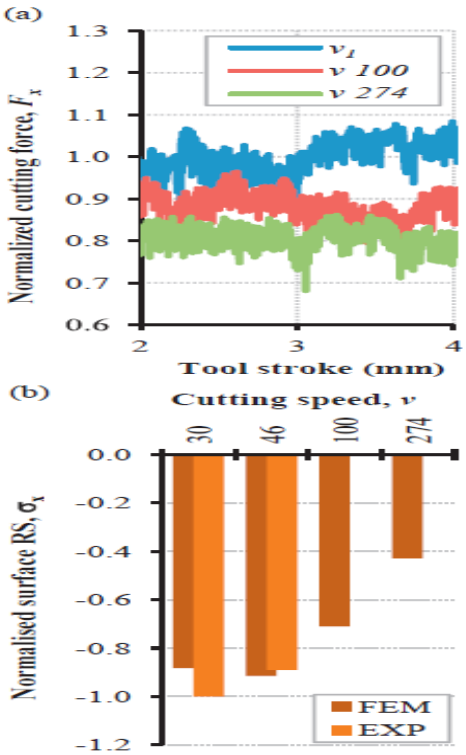

Fig. 13 (a) cutting force (Fx); (b) the surface residual stresses (σ_x) [1]

The cutting force was reduced slightly while compressive residual stresses decreased much with approximately 20% and 50% respectively, because of cutting speed increasing (at 100 and 274) m / min. Cutting force decrease is attributed to thermal softening of the material processed while the decrease of compression residual stresses is associated with the increase of temperature at processed surface. Some simulation that analyze the influence of cutting speed on the residual stresses, with a constant feed rate of 0.2 mm/rev and a tool rake angle of 6°, were performed by Stenberg and Proudian.

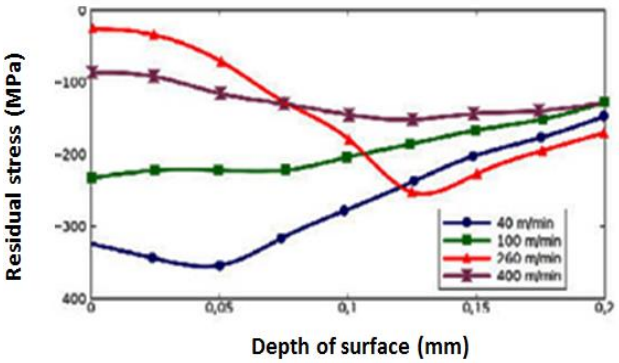

Fig. 14 Variation of residual stresses for different cutting speeds, feed rate 0.2mm / rev, departure angle 6° [43]

The influence of feed rate on the residual stresses is analyzed at a constant cutting speed of 260 m / min and a clearance angle of 6 °. The experimental results are shown in Figure 15 and the results of FEM simulation are displayed in Figure 16.

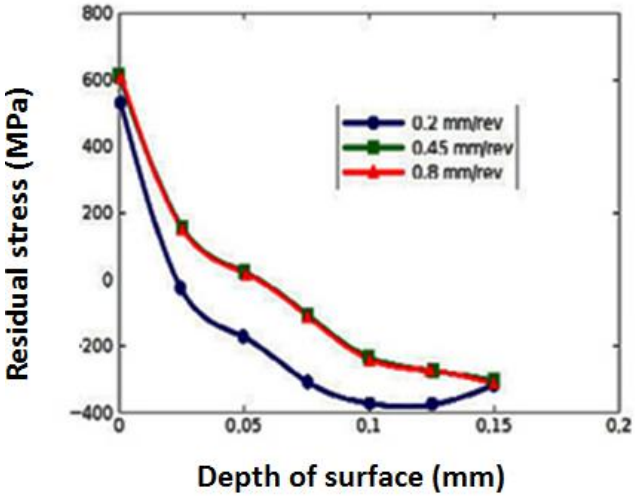

Fig.15 Variation of residual stresses for different feed rates (experimental results) [43]

6. INFLUENCE OF CUTTING TOOL GEOMETRY ON THE RESIDUAL STRESSES

The nature of tensile or compressive residual stress depends on the geometry of the cutting part of the tool [6] and on the machining parameters lick cutting speed, feed supply and departure angle. The analysis of residual stress generation by pure analytical methods [15] is difficul due to the complexity of physical training chip [25] and a variety of boundary conditions. An important role in the machining process simulation and analysis [10, 50] has the FEM analysis. The tensile residual stresses may result from the combination of mechanical and thermal effects.

Many authors have analyzed the influence of the tool edge radius in residual stresses generation. Nasr et al. [31, 48] showed that the tensile residual stresses level increases with rake angle, tool edge radius and feed rate.

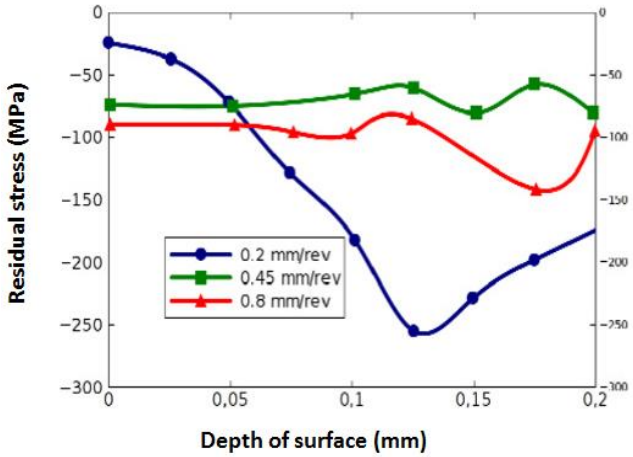

Fig.16 Variation of residual stresses for different feed rates (FEM simulation results) [43]

The analysis is performed for zero rake angle and through the increase of tool tip radius from 0.02 mm to 0.05 mm and 0.10 mm. Mechanical effects were analyzed by neglecting thermal expansion (Figure 17). The coefficient of friction is 0.2. The maximum σ11 is indicated by an arrow for each R value.

A beneficial effect seems to have the increasing of peak radius of the cutting. In case of speeds field analysis was observed an increase of the built-up with increasing peak radius of the cutting edge. The effect of built-up is beneficial in lowering the level of the tensile. If thermal expansion is considered, this leads to an increase of residual tensile level, (Figure 17b).

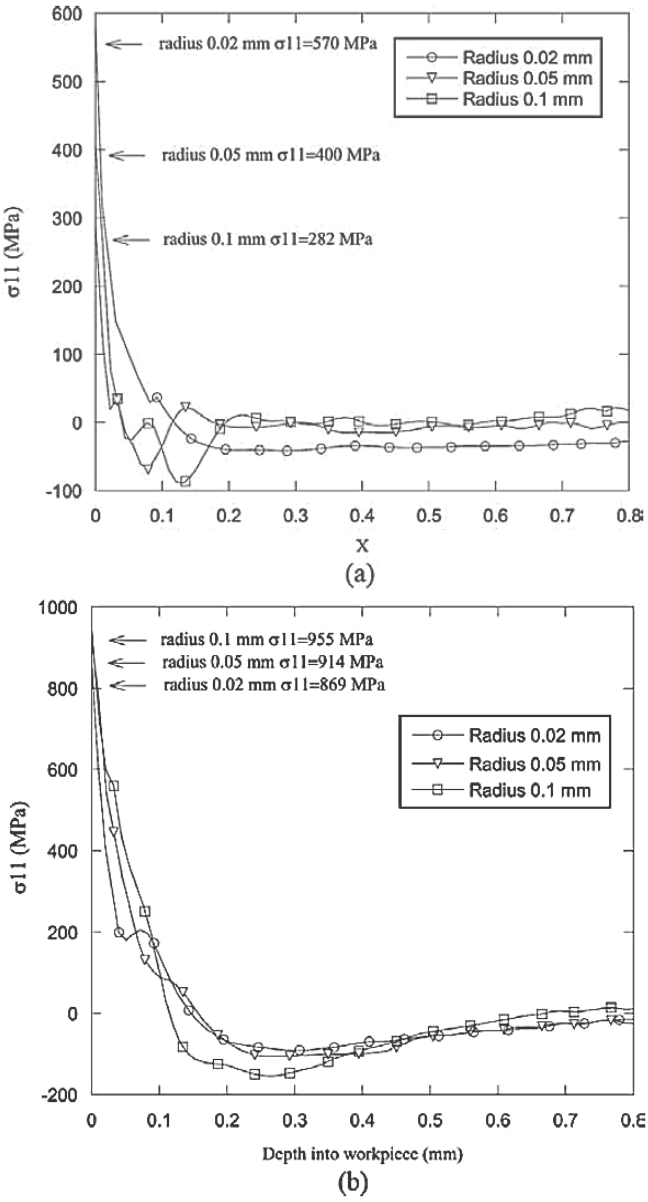

Fig.17 The influence of cutting edge radius (R = 0.02, 0.05 and 0.10 mm), on the residual stress σ11. (a) without thermal expansion and (b) with thermal expansion [25]

At high values of edge radius, tensile residual stresses are more pronounced because of increased surface temperature of the workpiece (Figure 18).

From carried out studies [1] was observed that the tool edge radius presents a significant influence on the residual stresses. Some cutting simulations were

performed at identical feed rate and the same cutting speeds, but radii rangi from 10 µm to 60 µm. Figure 19 show the edge radius effect on the prediction of cutting forces (Fx) and surface residual stress in cutting direction (x). Can be observed from figure that once with the increasing of edge radius (r), the cutting force increased slightly and the compression residual stresses decreases significantly.

For values of 20µm and 60µm of edge radius the compressive residual stresses decreased by approximately 25% and 60% respectively comparative with a edge radius of 10µm value. This decrease was associated with the substantial increasing of temperature in newly processed (generated) surface, Figure 20. Nasr et al. [29] was predicted the same tendency for orthogonal cutting of AISI 316 L stainless steel, for edge radiuses 20µm, in the contact area between tool and workpiece surface the additional heat generation increasing.

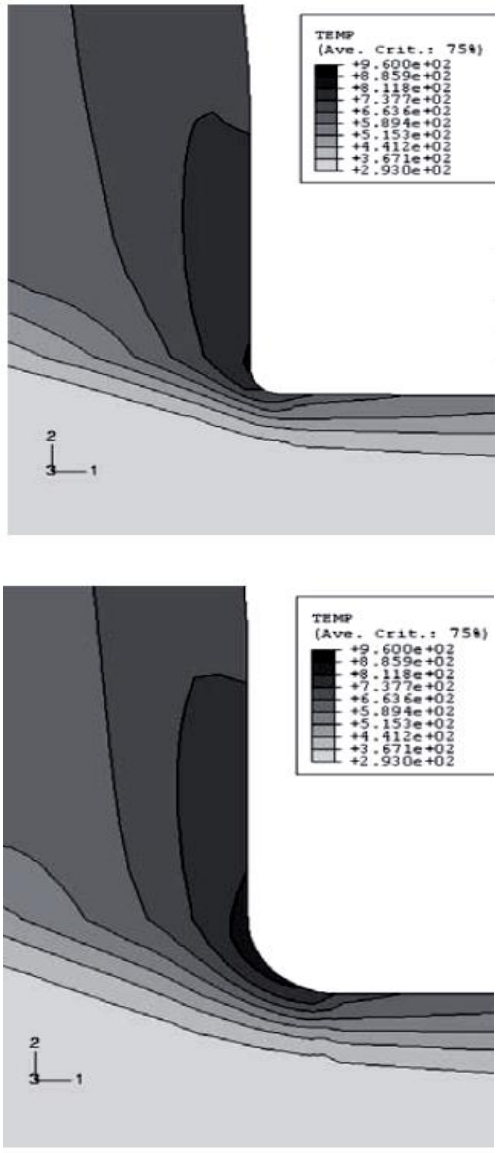

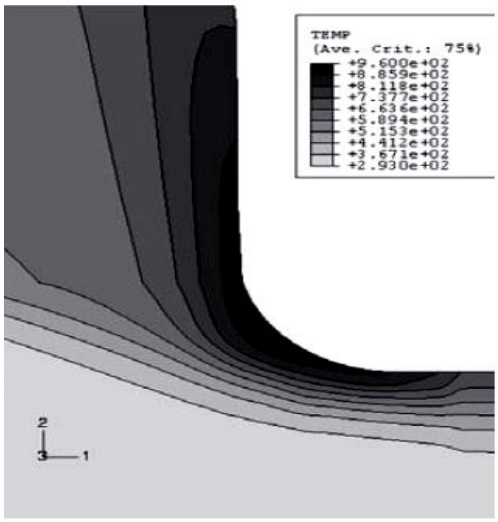

Fig. 18 K temperature domain while cutting for a tip radius of cutting edge of 0.05 mm, 0.10 mm and 0.15 mm [25]

A study of residual stresses at orthogonal machining of AISI 316L stainless steel, depending on the cutting edge radius of the cutting tool with 0.02mm, 0.03mm and 0.04mm values was presented by Maranhao et al. [19,20] (Figure 21). The value of cutting speed is 150 m / min, the friction coefficient of steel is 0.57, feed rate was 0.1 mm / rev and depth of cut 4mm. In the below chart it can be observed that the parameter does not significantly influence the residual stresses.

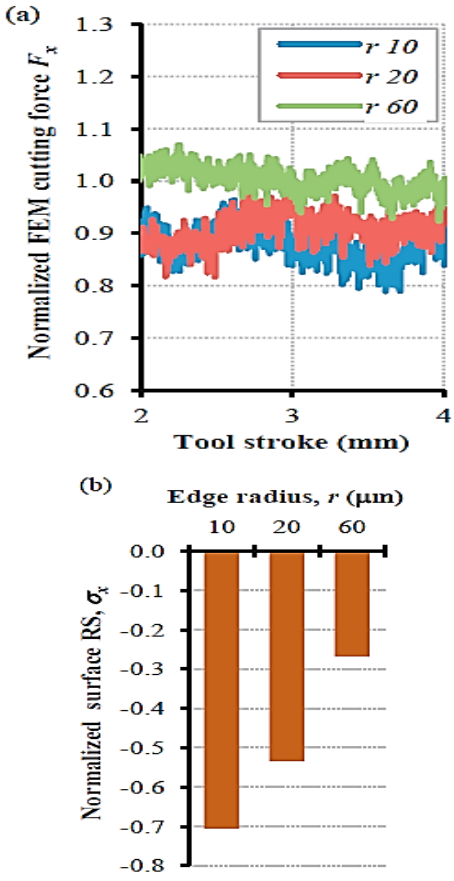

Fig. 19 (a) cutting force (Fx); (b) the surface residual stresses (σ_x),in the cutting direction [1]

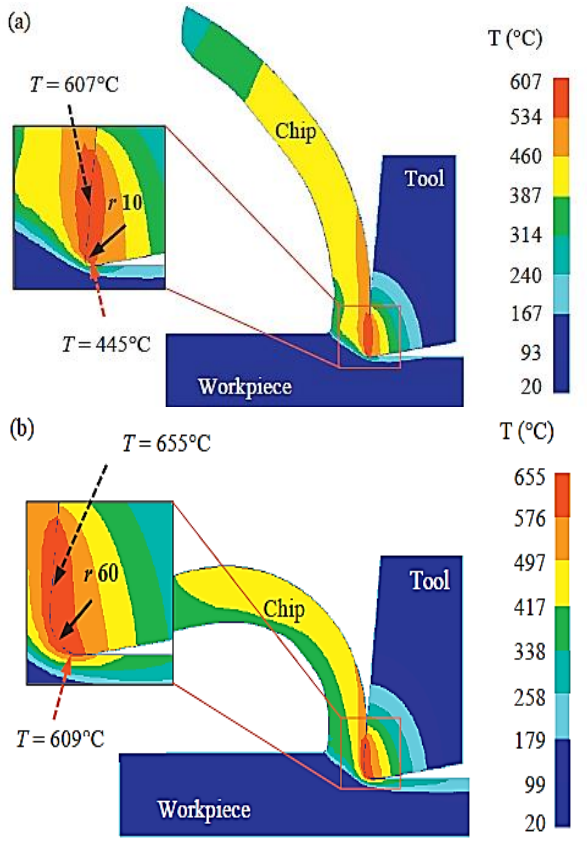

Fig. 20 The effect of edge radius (r) at the estimated temperature distribution in the shear zones: (a) r = 10 μm (b) r = 60 μm [1]

For the three values of the tool cutting edge radius tensile residual stresses are almost similar, compressive residual stress has also similar values and the affected layers have identical depth. Then, the residual stresses don't have a so great influence on radius peak [19]. Numerical model that analyze the effect of machining tool wear on the residual stress were developed and validated by Munoz-Sanchez et al. [28]. Some advantages of this model are: the ability to simulate a long length of the processed surface, low discretization distortions and time-efficient model.

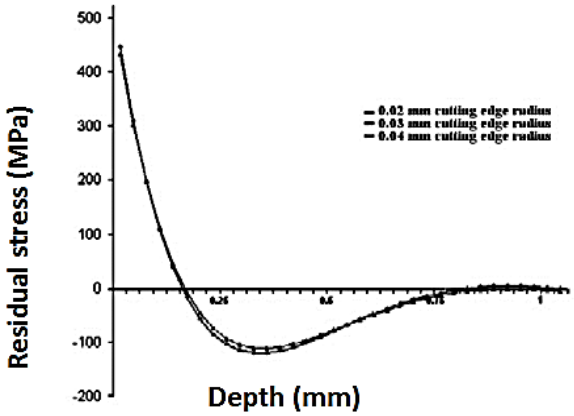

Fig .21 The distribution of residual stresses on the surface depth at orthogonal turning of AISI 316L stainless steel [19,20].

The validation of the model was was made with experimental tests performed with tools used. The model was used to estimate the residual stresses induced in Steel AISI 316 L and to reache a reasonable agreement with experimental results. FEM simulations that analyze the influence of cutting tool rake angle on residual stress (values of + 6 °, 0 ° and - 6 °, Figure 22, at a feed rate of 0.2mm / r and cutting speed of 260 m / min was conducted by Stenberg et al. [43]. at values of 0 ° and -6 can be observed that the departure angle residual stresses are tensile, at depths greater than material tending to zero. I case of positive rake angle (+ 6 °), residual stresses become compressive.

Lin et al. [16] have analyzed the influence of tool rake angle, making a comparation between the residual stresses generated with positive (+8 degrees.), 0° and negative (-6 degrees) tool rake angle. In the simulations performed the value of cutting speed was 2 m /s. Also the thermal expansion and the coefficient of friction, μ=0.2, are considered. In Figure 23 the maximum σ11 is indicated through an arrow for each value of rake angle.

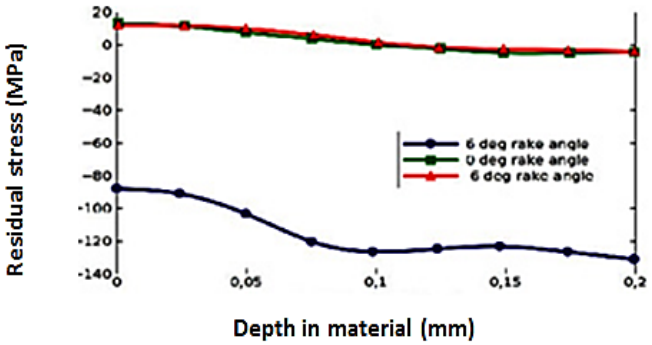

Fig. 22 Variation of of residual stresses for different cutting tool rake angle, (simulated results), [43]

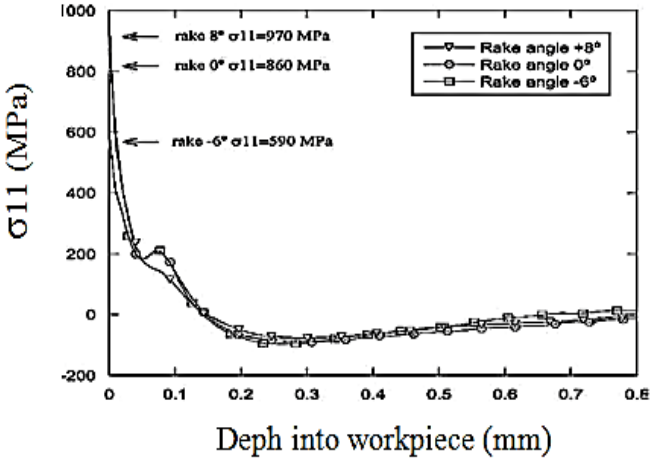

Fig. 23 The influence of tool rake angle on residual stress σ11, [25]

If the departure angle is negative (-6°), the maximum tensile residual stress (590 MPa) is lower and the compressive residual stress level increases. For the analysis of stress field σ11

during cutting when is taked into account the friction and the thermal expansion, the effect of cutting tool geometry tends to reduce tensile residual stresses for large negative values of departure angle. The effect of friction decreases the maximum value of the residual stress for any geometry of the tool. When the rake angles are small the temperature is increased. However, chips adherence on the tool rake face increases when the tool rake angle is lower, the built-up effect being improved. The result of the effect of built-up edge is to produce an "effective rake angle". This effective rake angle has to be lower than the actual rake angle and the level of the tensile residual stresses thus, is reduced. The reductions of tensile stresses when the rake angle is reduced solve the competition between these opposing effects. The results for the effect of rake angle on the residual stresses are useful at many industrial applications. It was observed that, usually, a positive rake angle generates machined surfaces with a higher quality than negative rake angles. Therefore, usually these types of tools are selected for finishing operations. when the concept of quality should include factors that influence the pieces duration of life, for example compressive residual stresses, a good choice is finishing operation with a negative rake angle. A study regarding the influence of rake angles on the residual stresses using various cutting tools, in the same cutting conditions of AISI 316L steel was conducted by Maranhao et al. [19]. The circumferential residual stress distribution along the depth of the blank's surface (obtained by numerical simulation with uncoated cutting tool clearance angles 0 ° and 15°) is presented in figure 24. The value of friction coefficient for steel is 0.57, depth of cut 4mm, the cutting speed has 150 m / min and feed rate was 0.1 mm / rev. In figure 24, can be observed that the residual stresses are not significantly influence by this parameter.

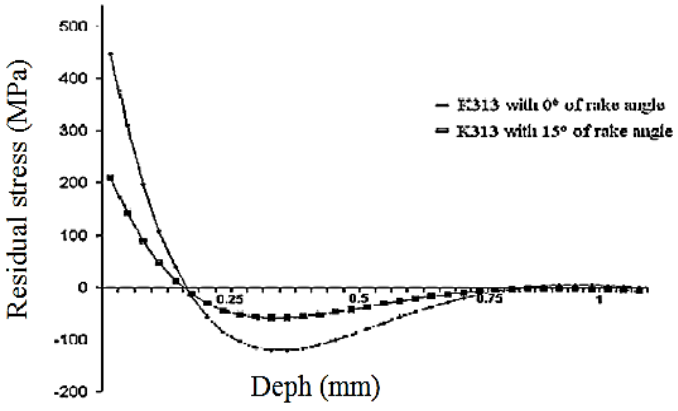

Fig. 24 Distribution of the residual stresses on at surface depth at orthogonal turning of AISI 316L stainless steel [19]

If both distributions are compare, a significant reduction of can be observed in the the workpiece surface when the cutting tool has a positive rake angle. The maximum tensile residual stress dropping from 450 MPa (for the tool cutting angle rake 0 °) to about 200 MPa (cutting tool with a rake angle of 15 °). For tensile residual stress distribution the layer thickness is the same for both types of cutting tools (about 0.156 mm) and for compressive residual stress distribution the thickness of layer is the same in both versions (about 0.75 mm). The values of maximum compressive residual stress achieved -100MPa when the rake angle of tool is 0° and about -50 MPa for at a rake angle of 15° [19].

7. INFLUENCE OF PROCESSED MATERIAL ON RESIDUAL STRESSES

The finite element method was used by Lin et al. [16], for determining the deformation field from the workpiece material. Analyzing the deformation field, to evaluate the residual stresses after the deformation of the material was used the concept of particle stream. A three-dimensional finite element model was also developed and the expected results were compared with those measured. A finite element model (FEM) for the black and white layer formation in orthogonal machining hardened of the AISI 52100 steel was presented by Umbrello [47]. According to the author, in order to validate the proposed strategy simulation to investigate the influence of microstructural change of the material on the residual stresses a series of experiments were conducted. As a main result, due to rapid heating and quenching the workpiece it was demonstrated that microstructural changes occur. More than that, it was observed that both effects lead to black and white layers that influence the residual stresses profile. To model the workpiece material was introduced the Johnson-Cook plasticity model. Also, at tool-splinter interface was assumed the Coulomb friction coefficient. The continuous machining process was shaped using two identical cutting tools. After stages and after cutting of relaxation of residual stress the profile of this was obtained. The predicted residual stresses profiles were in reasonable agreement with experimental results, according to the authors. Using an arbitrary Lagrangian-Eulerian (ALE) finite element approach, Miguelez et al. [26] describe the generation of residual stresses in orthogonal machining. The roles of thermal expansion, the coefficient Taylor Quinney (controls heat generated by the flow of plastic) and thermal softening point are treated individually. By assuming the dry chipping conditions and the Coulomb friction law as well the influence of friction is analyzed. Along the rake faces and tool place, the friction coefficient has a complex control efect to heat generation (frictional heating). Must be mentioned that, due to adherence the splinter has the tendency to remain on the cutting tool.

8. INFLUENCE OF PLASTIC DEFORMATION AND RESIDUAL STRESSES ON THE THERMAL EXPANSION

The thermal effects and the mechanical deformation can influence the both Residual stresses [25]. A direct effect on the level of tensile residual stresses has the increase of heat due to plastic deformation and friction. The tensile residual stresses level decreases due to the increasing of temperature thus, appearing the thermal softening. Another effect occurs after cooling, thermal expansion causing tensile residual stresses. First of all the influence of thermal expansion in the workpiece material have to be analyzed. Cutting speed is 120 m / min, rake angle is zero and the friction coefficient Coulumb is 0.2. These values are used in all simulations. Radial distribution of residual stresses (σ11) and axial (σ33) are calculated taking into consideration thermal expansion and then compared with the case where the thermal expansion coefficient is zero (Figure 25). In Figure 25 can be observed that tensile residual stresses are higher if the thermal expansion is taken into account. We see that the tensile residual stresses are still present near the processed surface when thermal expansion is zero.

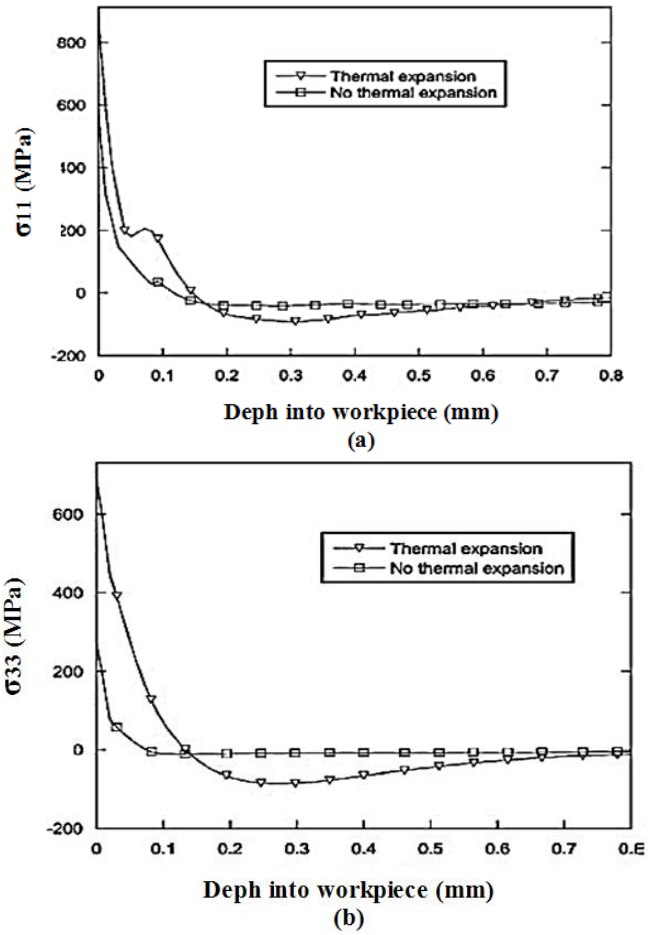

Fig. 25 Residual stress distribution obtained with and without thermal expansion: (a) σ11 and (b) σ33 [25]

9. THE INFLUENCE OF FRICTION ON RESIDUAL STRESSES

To analyze the influence of friction [25], the value of rake angle is zero, the coefficient of friction have different values μ = 0; 0.1; 0.2; 0.3 and 0.4. The simulations are performed at 2 m / s cutting speed, without thermal expansion (Figure 26a). The increase of friction in these conditions, decreases substantially the maximum level of tensile residual stress of the processed layer and has only a slight influence on the compressive residual stress. When thermal expansion is taken into account (Figure 26b), tensile residual stresses are enhanced due to the temperature growth due to friction. Can be observed a noticeable reduction of the residual tensile stress when the friction coefficient is higher. The maximum σ11 is indicated through an arrow for each value of friction coefficient.

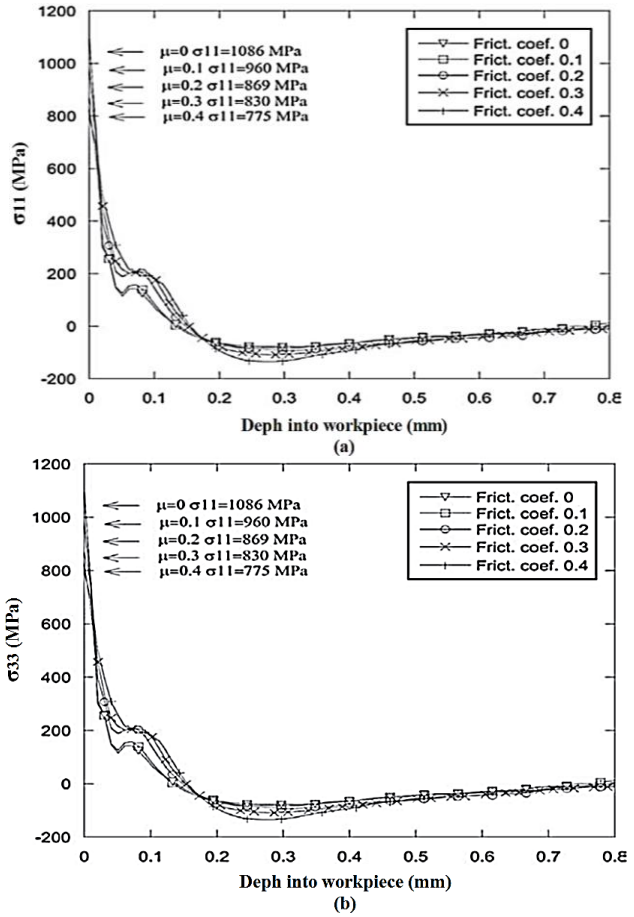

Fig. 26 The influence of of friction on residual stress σ11:
(a) without thermal expansion and
(b) with thermal expansion [25]

By changing the total amount of heat generated is analyzed the influence of thermal softening [25]. Quinney-Taylor coefficient values were artificially imposed at values of 0.6, 0.7 and 1.0. To isolate the thermal softening effect on residual stresses, the thermal expansion and friction are not considered.

Radial residual stress distributions σ11 (Figure 27) corresponding to simulation with negative rake angles (-6 º), shows that the higher Quinney - Taylor (QT) coefficients produce a decrease of tensile residual stress level. For axial residual stress σ33, same trend was observed.
The effect of a disappearance Quinney - Taylor coefficient was not studied because of unrealistic deformation of the chip without thermal softening. In In Figure 27, the maximum σ11 is indicated through an arrow for each value of QT coefficient.

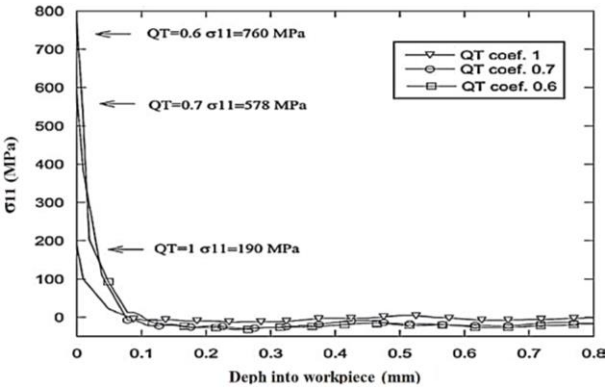

Fig. 27 Thermal softening effect on residual stresses σ11 through different values of Taylor-Quinney (QT) coefficient [25]

CONCLUSIONS

In machining, numerical modeling of residual stress was studied and analyzed since the last century. The modeling includes analytical methods, statistical, experimental and finite element methods. By previous research, significant parameters were identified that contribute of residual stress generation, are as follows :
- cutting parameters (cutting speed, feed rate, depth of cut);
- processing tool geometry (peak radius of cutting edge of tool, rake angle, rake face wear);
- behaviour of the workpiece material (its hardness) and the material of cutting tool.
In most previous research has concluded that the impact of mechanical, thermal loads has an important role in the generation of residual stress profile. Finite element method has been used in most recent studies, obtaining quite good results that estimate the residual stress generated due to cutting process. However, finite element analysis requires a sufficiently large time and a significant computing power. These aspects appear due to required change of working parameters during the cutting process. The new model selected for finite element simulation, must be recalculated, thus, increasing the working time.
After using finite element analysis method for the study of residual stress generated in material cutting machined parts, can be drawn the following conclusions:
- The qualitative estimation of residual stresses by finite element analysis method, led to an improvement in the process of cutting;
- 2D Simulation is fast and can be used for cutting processing simulation and for optimization of cutting parameters in terms of residual stress assessment;
-3D Simulation is more accurate but the computation time is greater. This offer a good comparison between cutting forces and thermal zones developed at machining. Results show that tensile residual stresses constantly appear on the surface processed and compressive residual stresses occur at a depth of 10 mm to 25 mm;
- main working parameters wich influence residual stresses are: feed rate, cutting depth, peak radius of cutting edge of tool and the cutting tool rake angle;
-In case of finishing operations with a tool sharp edges, the increasing of feed rate leads to the generation of compressive residual stresses, being significantly higher in the machined surface;
-at hard turning , for a couple of thermo-mechanical that is based on a finite element simulation, without explicit chip formation, cutting depth is the most important factor on residual stresses profile;
-for large radius of cutting edge of tool, high coefficients of friction between tool and workpiece material due to a high rake angle, a large coefficients of heat and increasing cutting speed significantly reduces the compressive residual stresses at the surface;
-The tensile residual stresses are influence by the complex interaction between mechanical and thermal effects. Has been shown that tensile stress is large when thermal expansion is increased and thermal softening is reduced. Mechanical effects can contribute to generate tensile residual stresses in the surface processed even in the absence of thermal expansion.

REFERENCES

1. Abboud, E., Shi, B., Attia, H., Thomson, V., Y. Mebrahtu, Y., (2013). *Finite element-based modeling of machining-induced residual stresses in Ti-6Al-4V under finish turning conditions*, Procedia CIRP 8, pp. 63-68.
2. Anurag, S., Guo, Y.B., Liu, Z. Q., (2010). *A new fem approach to predict residual stress profiles in hard turning without simulating chip formation*, Transactions of NAMRI/SME , Vol. 38.
3. Batalha, G.F., Delijaicov, S., Aguiar, J. B., Bordinassi, E.C., Stipkovic Filho, M., (2007). *Residual stresses modelling in hard turning and its correlation with the cutting forces*, Journal of Achievements in Materials and Manufacturing Engineering, Vol. 24, Issue 1.
4. Capello, E., (2005). // Journal of Materials Processing Technology 160**,** 221.

5.Chandrasekaran, H., M'Saoubi, R., Chazal, H., (2005). *Modelling of Material Flow Stress in Chip Formation Process from Orthogonal Milling and Split Hopkinson Bar Tests*, Mater. Sci. Technol., vol. 9, pp. 131–145.
6. Chen, L., El-Wardany, T. I., and W. C. Harris, W. C., (2004). *Modelling the Effects of Flank Wear Land and Chip Formation on Residual Stresses*, Ann. CIRP, vol. 53, no. 1, pp. 95–98.
7. Chen, L., et al., (2004). *Modelling the Effects of Flank Wear Land and Chip Formation on Residual Stresses*, CIRP Annals - Manufacturing Technology, vol. 53, pp. 95-98.
8. Cherng Su, J., (2006). *Residual stress modeling in machining processes*, A Dissertation Presented to The Academic Faculty, Georgia Institute of Technology.
9. Dolinsek, S., Ekinovic, S., Kopac, J., (2004). *A contribution to the understanding of chip formation mechanism in high speed cutting of hardened steel*, Journal of Materials Processing Technology, pp. 157-158, pp.485-490.
10. Ehmann, K. F., Kpoor, S. G., DeVor, R. E., Lazoglu, I., (2006). *Machining Processes Modelling: A Review*, J. Manuf. Sci. Eng. Trans. ASME, vol. 119, pp. 655–663, 2006.
11. Filice, L., Micari, F., Rizzuti, S., Umbrello, D., (2007). *A critical analysis on the friction modelling in orthogonal machining*, International Journal of Machine Tools and Manufacture 47, pp.709-714.
12. Grifiths, B. J., (2001). *Manufacturing Surface Technology – Surface Integrity & Functional Performance*, Prenton Press – Kogan Page Ltd., London, UK, 152-89.
13. Gunnberg, F., Escursell, M., Jacobson, M., (2006). // Journal ofMaterials ProcessingTechnology, 174 , 82.
14. Kopac, J., Stoic, A., Lucic, M., (2006). *Dynamic instability of the hard turning process*, Journal of Achievements in Materials and Manufacturing Engineering 18 (2006) 373-76.
15. Liang, S. Y., Su, J.-C., (2007). *Residual Stress Modeling in Orthogonal Machining*, Ann. CIRP, vol. 56, no. 1, pp. 65–68.
16. Lin, Z. C., Lin, Y. –Y., Liu, C. R., (1991). *Effect of Thermal Load and Mechanical Load on the Residual Stress of a Machined Workpiece*, International Journal ofMechanical Sciences, 33(4),pp. 263-278.
17. Liu, C.R. and Y.B. Guo, Y. B., (2000). *Finite Element Analysis of the Effect of Sequential Cuts and Tool-Chip Friction on Residual Stresses in a Machined Layer*, International Journal of Mechanical Sciences, 42(6), pp. 1069-1086.
18. Liu, M., Takagi, J. I., Tsukuda, A., (2004). *Effect of Tool Nose Radius and Tool Wear on Residual Stress Distribution in Hard Turning of Bearing Steel*, Journal ofMaterials Processing Technology, 2004. 150(3): pp. 234-241.
19. Maranhao, C., Davim, J. P., (2010). *Simulation Modelling and Theory*, 18, pp.139.
20. Maranhao, C., Davim, J. P., (2012). *Residual Stresses in Machining Using FEM Analysis -A Review*, Department of Mechanical Engineering, University of Aveiro, Campus Santiago, 3810-193, Aveiro, Portugal, Rev. Adv. Mater. Sci. 30, pp. 267-272.
21. Marusich, T.D., et al., (2003). *Three-Dimensional Finite Element Modeling of Hard Turning Processes*. Washington, DC., United States: American Society of Mechanical Engineers, New York, NY 10016-5990, United States.
22. Marusich, T.D., Usui, S., McDaniel, R.J., (2003) *Three-Dimensional Finite Element Prediction of Machining-Induced Stresses*, Washington, DC., United States: American Society of Mechanical Engineers, New York, NY 10016-5990, United States.
23. Merwin, J. E., Johnson, K.L., (1963). *An Analysis of Plastic Deformation in Rolling Contact*, Proceedings, Institution of Mechanical Engineers, London, 177(25): pp. 676-685.
24. Miguélez, H., Zaera, R., Rusinek, A., Moufki, A., Molinari, A., (2006). *Numerical Modelling of Orthogonal Cutting: Influence of Cutting Conditions and Separation Criterion*, J. Phys. IV, vol. 134, pp. 417–422.
25. Miguélez, M. H., Zaera, R., Molinari, A., Cheriguene, R., Rusinek, A., (2009). Residual stresses in orthogonal cutting of metals: the effect of thermo-mechanical coupling parameters and of friction, Published in: Journal of Thermal Stresses, vol. 32(3), pp. 269-289.
26. Miguelez, M. H., Zaera, R., Molinari, R. A., Cheriguene, R., Rusinek, A., (2009). // Journal of Thermal Stresses 32 , 269.
27. Mohammadpour, M., Razfar, M. R., Saffar, R. J., (2010). // Simulation Modelling and Theory 18, 378.
28. Munoz-Sanchez, A., Cantelli, J. A., Cantero, J. L., Miguelez, M. H., (2011) // Simulation Modelling and Theory 19 , 872.
29. Nasr, M. N. A., et al., (2007). *Modelling the effects of tool-edge radius on residual stresses when orthogonal cutting AISI 316L*. International Journal of Machine Tools and Manufacture, vol. 47, pp. 401-411.
30. Nasr, M. N. A., Ng, E. G., Elbestawi, M. A., (2008). //Finite Elements in Analysis and Design 44,149.
31. Nasr, M., Ng, E. G., Elbestawi, M. A., (2007). *Modelling the Effects of Tool-Edge Radius on Residual Stresses when Orthogonal Cutting AISI316L*, Inter. J. Mach. Tools Manuf.,vol. 47, pp. 401–411.
32. Okushima, K., Kakino, Y., (1971). *Residual Stress Produced by Metal Cutting*, CIRP Annals, 20(1): pp. 13-14.
33. Outeiro, J. C., Dias, A. M., Jawahir, I. S., (2006). *On the Effects of Residual Stresses Induced by Coated and Uncoated Cutting Tools with Finite Edge Radii in Turning Operations*, Annals of the CIRP

55(1), pp.111–116.
34. Outeiro, J. C., Dias, A. M., Lebrun, J. L., Astakhov, V. P., (2002). *Machining Residual Stresses in AISI 316L Steel and their Correlation with the Cutting Parameters*, Machining Science and Technology 6(2), pp.251–270.
35. Outeiro, J. C., Pina, J. C., M'Saoubi, R., Pusavec, F., Jawahir, I. S., (2008). *Analysis of residual stresses induced by dry turning of difficult-to-machine materials*, CIRP Annals-Manufacturing Technology 57, pp.77-80.
36. Outeiro, J. C., Umbrello, D., M'Saoubi, R., (2006). *Experimental and FEM Análisis of Cutting Sequence on Residual Stresses in Machined Layers of AISI 316L Steel*, Mater.Sci. Forum, vol. 524–525, pp. 179–184.
37. Outeiro, J. C., Umbrello, D., M'Saoubi, R., (2006). *Experimental and Numerical Modelling of the Residual Stresses Induced in Orthogonal Cutting of AISI 316L Steel*, International Journal of Machine Tools and Manufacture 46(14), pp.1786–1794.
38. Özel, T., (2006). *The influence of friction models on finite element simulations of machining*, International Journal of Machine Tools and Manufacture 46, pp.518-530.
39. Özel, T., Zeren, E., (2005). *Finite Element modelling of Stresses induced by High Speed Machining with Round Edge Cutting Tools*, ASME International Mechanical Engineering Congress and Exposition.
40. Özel, T., Zeren, E., (2006). *Finite Element Modelling of Stresses Induced by High Speed Machining with Round Edge Cutting Tools*. Proc. IMECE'05, Orlando, Florida, November 5–11.
41. Proudian, J., (2012), *Simulating residual stress in machining;from post process measurement to pre-process predictions*, A Thesis Submitted to The School of Industrial Engineering and Management of KTH Royal Institute of Technology, Stockholm.
42. Shi, B., et al., (2005). *Simulation of the Machining Process, Considering the Thermal Constriction Resistance of Multi-layer Coated Tools*, Proceeding of the 8th CIRP International Workshop on Modeling of Machining Operations, Chemnitz, Germany.
43. Stenberg, N., Proudian, J., (2013). *Numerical modelling of turning to find residual stresses*, 14th CIRP Conference on Modeling of Machining Operations (CIRP CMMO), Procedia CIRP 8, pp.258–264.
44. Thiele, J. D., Melkote, S. N., (1999). *Effect of Tool Edge Geometry on Workpiece Sub-Surface Deformation and through-Thickness Residual Stresses for Hard-Turning of AISI 52100 Steel*, Technical Paper-Society of Manufacturing Engineers. MR,(MR99-167), pp.1-6.
45. Tönshoff, H.K., Wobker, H. G., Brandt, D., (1995). *Hard turning - influence on the workpiece properties*, Transactions of the NAMRI/SME 23, pp. 215–20.
46. Tsuchida, K., Kawada, Y., Kodama, S., (1975). *Study on the Residual Stress Distributions by Turning*, 18(116): pp. 123-130.
47. Umbrello, D., (2011). // International Journal of Advanced Manufacturing Technology, 54, 887.
48. Umbrello, D., M'Saoubi, R., Outeiro, J. C., (2007). *The Influence of Johnson–Cook Material Constants on Finite Element Simulation of Machining of AISI 316L Steel*, Int. J. Mach. Tools Manuf., vol. 47, pp. 462–470.
49. Umbrello, D., Outeiro, J. C., M`Saoubi, R., Jayal, A. D., I. S. Jawahir, I. S., (2010). // CIRP Annals Manufacturing Technology 59, 113.
50. Vaz, Jr. M., Owen, D. R. J., Kalhori, V., Lundblad, M., Lindgren, L.-E., (2007). *Modelling and Simulation of Machining Processes*, Arch. Comput. Meth. Eng., vol. 14, pp. 173–204.
51. Wiesner, C., (1992). *Residual Stresses after Orthogonal Machining of AISI 304: Numerical Calculation of the Thermal Component and Comparison with Experimental Results*. Metallurgical Transactions A (Physical Metallurgy and Materials Science), 23A(3): p. 989-996.
52. Zong, W. J., Sun, T., Li, D., Cheng, K., Liang, Y. C., (2006). *FEM optimization of tool geometry based on the machined near surface's residual stresses generated in diamond turning*, Journal of Materials Processing Technology 180, 271-78.
53. http://ccimn.ulbsibiu.ro/mef.pdf Accesed: 12.06.2014.
54. Hearn, E. J. , (1997), *Residual stresses In Mechanics of Materials 2: An Introduction to the Mechanics of Elastic and Plastic Deformation of Solids and Structural Materials*. Vol. 2 394-408 Butterworth-Heinemann Oxford.
55. Salio, M., Berruti, T., De Poli, G., (2006), *Prediction of Residual Stress Distribution Alter Turning in Turbine Disks*, Int. J. Mech. Sci., vol. 48, pp. 976–984.
56. Outeiro, J. C., Dias, A. M., (2006*), Influence of Work Material Properties on Residual Stresses and Work Hardening Induced by Machining*, Mater. Sci. Forum, vol. 524–525, pp. 575–580.
57. M'Saoubi, R., Outeiro, J. C., Changeux, B., Lebrun, J. L., Moräo Dias, A., (1999), *Residual Stress Analysis in Orthogonal Machining of Standard and Resulfurized AISI 316L Steels*, J. Mater. Proc. Tech., vol. 96, pp. 225–233.
58. Mishra, A. and T. Prasad, (1985) *Residual Stresses Due to a Moving Heat Source*, International Journal of Mechanical Sciences, 27(9): p. 571-581.
59. Abrao, A. M., Aspinwall, D., (1996). *The surface integrity of turned and ground hardened bearing steel*, Wear 196, 279-84.

Received: May 15, 2014 / Accepted: December 10, 2014 / Paper available online: December 15, 2014